Analyst

RSC Publishing

PAPER

View Article Online
View Journal | View Issue

Cite this: *Analyst*, 2013, **138**, 3490

Metal–organic frameworks-based biosensor for sequence-specific recognition of double-stranded DNA

Lifen Chen,[a] Hanye Zheng,[b] Xi Zhu,[b] Zhenyu Lin,*[b] Longhua Guo,[b] Bin Qiu,[b] Guonan Chen[b] and Zhong-Ning Chen*[a]

Received 2nd March 2013
Accepted 2nd April 2013

DOI: 10.1039/c3an00426k

www.rsc.org/analyst

A simple, cost-efficient, sensitive and selective fluorescence sensor is developed for sequence-specific recognition of duplex DNA (ds-DNA) *in vitro* using metal–organic framework (MOF) as the sensing platform. *N*,*N*-Bis(2-hydroxy-ethyl)dithiooxamidatocopper(II) (H_2dtoaCu) was chosen as the example MOF, because it strongly chemisorbs the dye-labeled probe TFO (triplex-forming oligonucleotide), and quenches fluorescence from the dye. In the presence of target ds-DNA (the PPT of HIV RNA, a 16-bp ds-DNA sequence), the TFO could interact with the major groove in ds-DNA (*via* Hoogsteen hydrogen bonding) to form a rigid triplex structure, resulting in fluorescence recovery. The enhanced fluorescence signal has a relationship with the ds-DNA concentration, the detection limit is as low as 1.3 nmol L^{-1} ($S/N = 3$) with good selectivity, which is lower than that based on a graphene oxide platform and electrochemical-DNA sensor.

1 Introduction

Since the first case reported in 1981, immunodeficiency virus type 1 (HIV-1) has infected and resulted in the death of millions of people. It is known that the polypurine tract sequence (PPT) of HIV-1 RNA plays an important role in the viral life-cycle.[1–3] PPT can create a RNA primer on the DNA terminus strand because of its resistance to RNase H activity of the reverse transcriptase. Hence, analysis of the proviral DNA sequence corresponding to PPT of HIV RNA is very important in clinical diagnostics and treatment.[4]

Generally, classical DNA detection is based on hybridization of complementary single-strand DNA with each other.[5,6] This method requires the generation of single-stranded DNA prior to analysis.[7] Recently, triplex DNA technology has attracted considerable attention. The triplex-forming oligonucleotide (TFO) can interact with the major groove in ds-DNA to form a rigid triplex structure *via* Hoogsteen hydrogen bonding or reverse Hoogsteen hydrogen bonding.[8,9] Many biosensors have been developed based on this principle. For example, Patterson *et al.* developed a reagentless, electrochemical biosensor for double-stranded DNA detection using a triplex-forming oligonucleotide as the probe.[7] Zhu *et al.* reported a gold nanoparticle-based colorimetric assay for single-nucleotide polymorphism of triplex DNA.[10] These methods show that ds-DNA can be detected *in vitro* directly without cumbersome pretreatment processes.

Metal–organic frameworks (MOFs) are materials which consist of metal ions or clusters connected by organic linker groups. MOFs have the advantages of flexible porosity, high surface area and well-defined configuration.[11,12] Correspondingly, MOFs have a wide range of applications in many fields, such as gas storage,[13,14] heterogeneous catalysis,[15] separations,[16–18] and drug delivery.[19] In this study, we utilize MOF as the sensing platform to detect ds-DNA (HIV 16-bp oligopyrimidine·oligopurine proviral DNA) *in vitro*. *N*,*N*′-Bis(2-hydroxyethyl)dithiooxamidatocopper(II) (H_2dtoaCu) was chosen as an example, because it possesses a two-dimensional sheet structure, the parallel H_2dtoaCu is connected by intermolecular hydrogen bonds, and the Cu^{2+} ion is surrounded by two S, two N, and one Cu atoms. The schematic diagram of this senor is shown in Scheme 1. H_2dtoaCu contains stacking π-electron systems of the bridging ligand dithiooxamide and the d^9 metal center Cu^{2+}, which strongly absorbs fluorescein amidite (FAM)-labeled TFO and quenches fluorescence of FAM due to the photoinduced electron transfer (PET) process.[20] After addition of the target ds-DNA, TFO interacted with the bases in the major groove of the target ds-DNA to form a rigid triplex structure *via* Hoogsteen hydrogen bonds.[21] This interaction will alter the configuration between the probe TFO and H_2dtoaCu, and make the probe TFO release from the H_2dtoaCu surface, resulting in recovery of fluorescence. Enhancement of the fluorescence intensity is related to the concentration of the target ds-DNA.

[a]*State Key Laboratory of Structural Chemistry, Fujian Institute of Research on the Structure of Matter, Chinese Academy of Sciences, Fuzhou, Fujian 350002, China. E-mail: czn@fjirsm.ac.cn; Fax: +86-591-83792346*

[b]*MOE Key Laboratory of Analysis and Detection for Food Safety, Fujian Provincial Key Laboratory of Analysis and Detection Technology for Food Safety, Department of Chemistry, Fuzhou University, Fuzhou, 350002, China. E-mail: zylin@fzu.edu.cn*

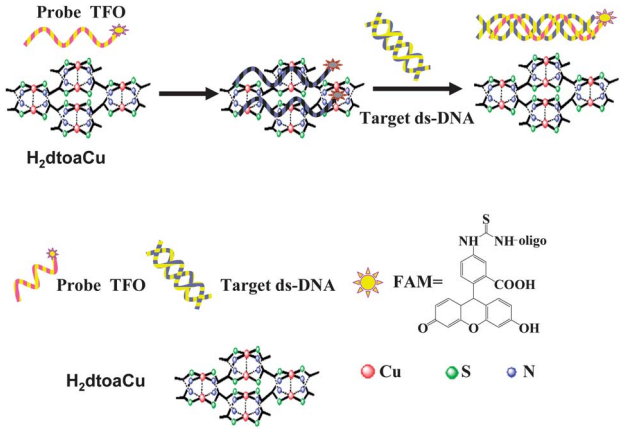

Scheme 1 Mechanism for the ds-DNA fluorescent biosensor based on MOF.

2 Experimental

2.1 Apparatus and chemicals

DNA sequences were synthesized by Sangon Inc. (Shanghai, China) and are shown as follows:[10]

Probe TFO-1: 5′-FAM-TTCTTCTTTTTTCT-3′
Complementary target duplex DNA (dsDNA-1,2)
DNA-1: 5′-CGA GTT AAG AAG AAA AAA GAT TGA GC-3′
DNA-2: 5′-GCT CAA TCT TTT TTC TTC TTA ACT CG-3′
Mutated duplex DNA (ds-DNA-3,4,5,6)
One base pair mutated:
DNA-3: 5′-CGA GTT AAG AAA AAA AAA GAT TGA GC-3′
DNA-4: 5′-GCT CAA TCT TTT TTT TTC TTA ACT CG-3′
Two base pair mutated:
DNA-5: 5′-CGA GTT AAG AAA AAA AAG GAT TGA GC-3′
DNA-6: 5′-GCT CAA TCC TTT TTT TTC TTA ACT CG-3′
Complementary ss-DNA:
DNA-7: 5′-AGA AAA AAG AAG AA-3′
Non-specific ss-DNA:
DNA-8: 5′-CGA GGC GAT GCC GAA CTC GA-3′.

All DNA samples were dissolved in Tris–HCl buffer solution (pH = 7.4, 100 mmol L^{-1} NaCl, 10 mmol L^{-1} KCl, 10 mmol L^{-1} $MgCl_2$) and stored at 4 °C for use.

H_2dtoaCu was synthesized according to the published procedure.[22,23] 1.0 mg H_2dtoaCu powder was dispersed into 1.0 mL double-distilled water with oscillation and ultrasound to form 1.0 mg mL^{-1} MOF aqueous solution and then stored at 4 °C for later use. All other chemicals employed were all of analytical grade.

Cary Eclipse Fluorescence Spectrophotometer (Varian Corporation, USA) was used for the fluorescent measurements. The apparatus parameters were set as follows: λ_{ex} = 480 nm (slit 10 nm), λ_{em} = 490–600 nm (slit 10 nm). Fluorescence intensity at 518 nm was used to quantitative analysis.

2.2 Preparation of target duplex DNA

Duplex DNA (dsDNA-1,2) was prepared according to the previous reports.[10] Briefly, DNA-1 and DNA-2 (1 : 1 5 μmol L^{-1} for each, containing 10 mmol L^{-1} $MgCl_2$) were incubated at 95 °C for 5 min, and oscillated at 35 °C for 3 h. The resulting solution was stored at 4 °C for later use.

2.3 Assay of target duplex DNA

First, 20 μL of H_2dtoaCu 1 mg mL^{-1} aqueous solution was incubated with 50 nmol L^{-1} probe TFO at room temperature and oscillated to form TFO–H_2dtoaCu complex. The fluorescence intensity of the solution was detected, then different concentrations of targets were added into the solution containing TFO–H_2dtoaCu complex with oscillation at 35 °C for 3 h (except for the time-course study). The complex obtained was used immediately to measure fluorescence.

3 Results and discussion

3.1 Mechanisms of triplex DNA-based biosensor

A simple experiment verified our hypothesis. Fig. 1 showed the fluorescence emission spectra of probe TFO under different conditions. The fluorescence spectrum of probe TFO (curve a) showed strong fluorescence emission. However, in the presence of H_2dtoaCu, up to 81% quenching of the fluorescence emission was observed (curve c). The quenching efficiency (Q_E, %) of probe TFO was calculated using the formula: $Q_E = (F_0 - F_M)/F_0 \times 100\%$, where F_M and F_0 are fluorescence intensity at 518 nm in the presence and absence of H_2dtoaCu. Meanwhile, the TFO–H_2dtoaCu complex had significant fluorescence enhancement upon the addition of complementary target ds-DNA (curve b).

As shown in Table 1, Cu^{2+} could quench the fluorescence of probe TFO and the quenching efficiency (Q_E, %) reached 88.7%. Dithiooxamide had less fluorescence quenching capacity. After addition of target ds-DNA neither showed fluorescence recovery. The reason for this can be ascribed to the interaction between TFO and Cu–TFO complex, which is stronger than the target ds-DNA–TFO, therefore the target ds-DNA does not release TFO from the Cu–TFO complex and the fluorescence signal does not recover. The addition of target ds-DNA released TFO from the H_2dtoaCu sensing platform due to the TFO being adsorbed on H_2dtoaCu. The interaction between ds-DNA–TFO

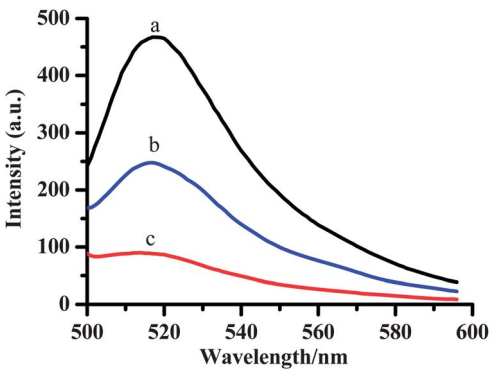

Fig. 1 Fluorescence emission spectra of probe TFO (50 nmol L^{-1}) at different conditions: (a) probe TFO in the absence of H_2dtoaCu, (b) probe TFO + 0.06 mg mL^{-1} H_2dtoaCu + 500 nmol L^{-1} target ds-DNA, (c) probe TFO in the presence of 0.06 mg mL^{-1} H_2dtoaCu.

Table 1 Fluorescence intensity changes with different kinds of quencher

	$CuSO_4 \cdot 5H_2O$	H_2dtoaH_2	$H_2dtoaCu$
F_0 (FAM–DNA)	486	497	467
F_M (FAM–DNA + quencher)	55	474	90
F_T (FAM–DNA + quencher + ds-DNA)	50	480	247
$Q_E\%$ $(1 - F_M/F_0)$	88.7%	0.046%	80.7%
$F_T - F_M$	−5	6	157

is higher than TFO–MOF. Accordingly, we infer that Cu^{2+} in $H_2dtoaCu$ is the critical quenching factor, the reason for this may be due to the d^9 configuration of Cu^{2+} triggering a photo-induced electron transfer (PET) process.[20]

3.2 Optimization of condition and dynamic studies of the sensor

The effect of the dosage of $H_2dtoaCu$ was studied (Fig. 2(A)). The fluorescence intensity of 50 nmol L^{-1} probe TFO (25 μL of 1 μmol L^{-1} probe TFO) decreased with increasing MOF dosage from 0–20 μL (the concentration of $H_2dtoaCu$ was 1 mg mL^{-1}) and then reached a plateau. When 20 μL $H_2dtoaCu$ was added, about 80% of fluorescence emission quenching was observed. Hence, 20 μL $H_2dtoaCu$ was chosen for following experiment.

The dynamic behavior of TFO–$H_2dtoaCu$ was studied by monitoring the changes of fluorescence intensity with time. Fig. 2(B) shows fluorescence recovery of TFO–$H_2dtoaCu$ in the presence of ds-DNA as a function of incubation time. With increase of incubation time, fluorescence intensity increased gradually and reached a platform after 3 h. Hence, 3 h was chosen as the optimum incubation time.

3.3 Quantitative analysis of the target ds-DNA

Fig. 3(A) characterized the fluorescence emission spectra of the FAM-labeled TFO–$H_2dtoaCu$ complex upon addition of different concentrations of ds-DNA. Increasing the target ds-DNA concentration caused a gradual increase in fluorescence intensity implying that more TFO was released from $H_2dtoaCu$. Fig. 3(B) shows a linear relationship between the fluorescence change $(F_T - F_M)/F_M$ and the concentration of target ds-DNA in the range 4 nM to 200 nM, where F_M and F_T were fluorescence intensities at 518 nm in the absence and presence of target ds-DNA and after the introduction of $H_2dtoaCu$ calculated by:

$$R_E = 0.0019c + 0.2382,\ R = 0.9952$$

where c is the concentrations of target ds-DNA, and R_E is the fluorescence change using the formula: $R_E = (F_T - F_M)/F_M$. R is the regression coefficient of the equation. Based on this method, the detection limit of ds-DNA was estimated to be 1.3 nmol L^{-1} (defined as $S/N = 3$), which is lower than that based on a graphene oxide platform and the electrochemical-DNA sensor.[24,7] In addition, five newly prepared ds-DNA solutions (40 nmol L^{-1}) were used as a parallel experiment. It was found that the relative standard deviation (RSD) was 5.34%, which indicated that this method has good repeatability.

3.4 Sequence selectivity of the assay

To authenticate the specificity of the sensing platform, we chose the same concentration of different targets (one base pair mutated ds-DNA, two base pair mutated ds-DNA and the complemental ss-DNA) to hybridize with probe TFO. Target ds-DNA combines with probe TFO through the formation of C^+GC and TAT triads, where the GC base pair is recognized by the C base and forms a C^+GC triad. The AT base pair is recognized by the T base and forms a TAT triad. Fig. 4 in the presence of one base pair mutated ds-DNA (one GC base pair was replaced with AT) or two base pair mutated ds-DNA (two base pair were replaced) shows that fluorescent recovery is not obvious and indicates lower $(F_T - F_M)/F_M$ due to the unstable existence of the

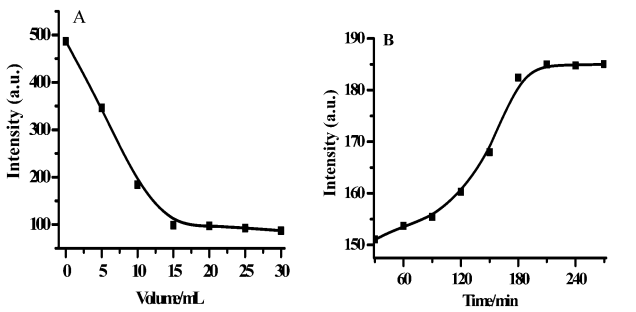

Fig. 2 (A) Effect of dosage of $H_2dtoaCu$ on fluorescence intensity of the system at 50 nmol L^{-1} TFO (25 μL of 1 μmol L^{-1} probe TFO). (B) Influence of incubation time between the TFO–$H_2dtoaCu$ complex and the target ds-DNA on fluorescence intensity. Concentration: [$H_2dtoaCu$] = 0.06 mg mL^{-1}, [probe TFO] = 50 nmol L^{-1}, [target ds-DNA] = 200 nmol L^{-1}. The fluorescence intensity is collected at 518 nm.

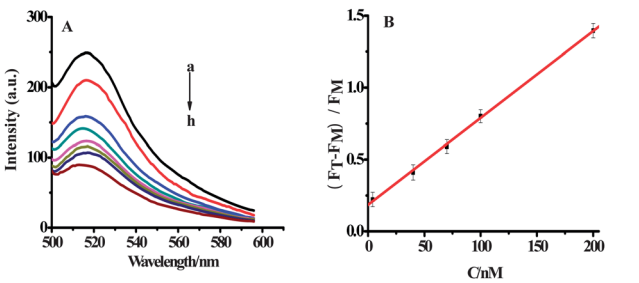

Fig. 3 (A) Fluorescent curves after incubation with varying concentrations of ds-DNA at room temperature. (a) 500 nmol L^{-1}; (b) 200 nmol L^{-1}; (c) 100 nmol L^{-1}; (d) 70 nmol L^{-1}; (e) 40 nmol L^{-1}; (f) 20 nmol L^{-1}; (g) 4 nmol L^{-1}; (h) 0 nmol L^{-1}. (B) Plot of $(F_T - F_M)/F_M$ *versus* ds-DNA concentrations. [probe TFO] = 50 nmol L^{-1}, [MOF] = 0.06 mg mL^{-1} incubation time = 180 min.

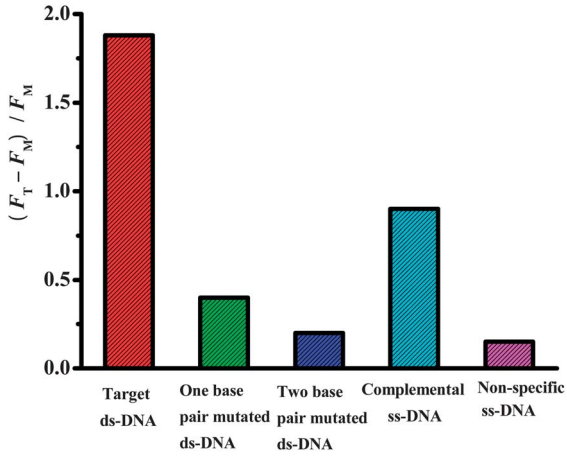

Fig. 4 Fluorescence intensity changes $(F_T - F_M)/F_M$ of the FAM-labeled TFO–H_2dtoaCu toward target ds-DNA, one base pair mutated ds-DNA, two base pair mutated ds-DNA, complemental ss-DNA and non-specific ss-DNA. The concentration of ds-DNA and complemental ss-DNA 1 μmol L^{-1}, the concentration of the non-specific ss-DNA is 25 μmol L^{-1}. F_M and F_T are fluorescence intensities at 518 nm in the absence and presence of targets after the introduction of H_2dtoaCu.

CAT and TGC triads. However, the introduction of complete complementary target ds-DNA or ss-DNA sequence results in significant fluorescence enhancement and larger $(F_T - F_M)/F_M$. In the presence of higher concentrations of non-specific ss-DNA (25 μmol L^{-1}) there is little change in the fluorescence. These results indicate that the sensing platform performs favorably with good specificity for the detection of ds-DNA *in vitro*.

4 Conclusions

In summary, we have successfully developed a cost-efficient simple and sensitive fluorescent biosensor for HIV DNA based on triplex-DNA technology. We used H_2dtoaCu as a detecting platform, which acted to absorb probe TFO and quench fluorescence intensity. Upon the addition of the target ds-DNA, probe TFO was released from the platform and fluorescence is recovered. Based on this approach, the detection limit of HIV DNA is 1.3 nmol L^{-1}. This indicates that MOFs as a new platform can substitute for GO and SWCNT for the detection of biomolecules.

Acknowledgements

The authors thank the NSFC for Excellent Youth Scholars of China (21222506), NSFC (21175024, 41076059) and the Program for New Century Excellent Talents in University (NCET-12-0619) for their financial support.

References

1 A. J. Rattray and J. J. Champoux, *J. Virol.*, 1987, **61**, 2843–2851.
2 R. Resnick, C. A. Omer and A. J. Faras, *J. Virol.*, 1984, **51**, 813–821.
3 J. K. Smith, A. Cywinski and J. M. Taylor, *J. Virol.*, 1984, **49**, 200–204.
4 C. Escude, C. H. Nguyen, S. Kukreti, Y. Janin, J. S. Sun, E. Bisagni, T. Garestier and C. Helencad, *Proc. Natl. Acad. Sci. U. S. A.*, 1998, **95**, 3591–3596.
5 H. G. Parka, J. Y. Songa, K. H. Parka and M. H. Kim, *Chem. Eng. Sci.*, 2006, **61**, 954–965.
6 T. R. Nataša, J. Danica, N. K. Zora and N. V. Dragica, *Exp. Mol. Pathol.*, 2007, **82**, 262–268.
7 A. Patterson, F. Caprio, A. Vallée-Bélisle, D. Moscone, K. W. Plaxco, G. Palleschi and F. Ricci, *Anal. Chem.*, 2010, **82**, 9109–9115.
8 H. E. Moser and P. B. Dervan, *Science*, 1987, **238**, 645–650.
9 K. Hoogsteen, *Acta Crystallogr.*, 1959, **12**, 822–823.
10 X. L. Zhu, Y. x. Liu, J. H. Yang, Z. Q. Liang and G. X. Li, *Biosens. Bioelectron.*, 2010, **25**, 2135–2139.
11 P. Horcajada, R. Gref, T. Baati, P. K. Allan, G. Maurin and P. Couvreur, *Chem. Rev.*, 2012, **112**, 1232–1268.
12 C. A. Bauer, T. V. Timofeeva, T. B. Settersten, B. D. Patterson, V. H. Liu and B. A. Simmons, *J. Am. Chem. Soc.*, 2007, **129**, 7136–7144.
13 D. J. Collins and H. C. Zhou, *J. Mater. Chem.*, 2007, **17**, 3154–3160.
14 J. R. Li, M. Y. McCarthy, M. C. Sculley, J. Yu, J. Jeong, H. K. Balbuena, P. B. Zhou and H. C. Coord, *Chem. Rev.*, 2011, **255**, 1791–1823.
15 J. Lee, O. K. Farha, J. Roberts, K. A. Scheidt, S. T. Nguyen and J. T. Hupp, *Chem. Soc. Rev.*, 2009, **38**, 1450–1459.
16 E. Y. Lee and M. P. Suh, *Angew. Chem., Int. Ed.*, 2004, **43**, 2798–2801.
17 R. Kitaura, K. Fujimoto, S. I. Noro, M. Kondo and S. Kitagawa, *Angew. Chem., Int. Ed.*, 2002, **41**, 133–135.
18 B. L. Chen, C. D. Liang, J. Yang, D. S. Contreras, Y. L. Clancy, E. B. Lobkovsky, O. M. Yaghi and S. Dai, *Angew. Chem., Int. Ed.*, 2006, **45**, 1390–1393.
19 P. Horcajada, C. Serre, M. Vallet-Regi, M. Seban, F. Taulelle and G. Ferey, *Angew. Chem., Int. Ed.*, 2006, **45**, 5974–5978.
20 A. P. de Silva, H. Q. N. Gunaratne, T. Gunnlaugsson, A. J. M. Huxley, C. P. McCoy, J. T. Rademacher and T. E. Rice, *Chem. Rev.*, 1997, **97**, 1515–1566.
21 H. Kaur, B. R. Babu and S. Maiti, *Chem. Rev.*, 2007, **107**, 4672–4697.
22 S. Kanda, K. Ito and T. Nogaito, *J. Polym. Sci., Part A-1: Polym. Chem.*, 1967, **17**, 151–152.
23 S. Kanda, K. Yamashita and K. Ohkawa, *Bull. Chem. Soc. Jpn.*, 1979, **52**, 3296–3297.
24 C. K. Wu, Y. M. Zhou, X. M. Miao and L. S. Ling, *Analyst*, 2011, **136**, 2106–2110.